Thermochimica Acta 534 (2012) 64–70

Contents lists available at SciVerse ScienceDirect

Thermochimica Acta

journal homepage: www.elsevier.com/locate/tca

Kinetic studies on the thermal decomposition of aluminium doped sodium oxalate under isothermal conditions

M. Jose John, K. Muraleedharan, M.P. Kannan, V.M. Abdul Mujeeb, T. Ganga Devi*

Department of Chemistry, University of Calicut, Kerala 673 635, India

ARTICLE INFO

Article history:
Received 13 October 2011
Received in revised form 28 January 2012
Accepted 1 February 2012
Available online 10 February 2012

Keywords:
Aluminium doping
Contracting cylinder equation
Diffusion controlled mechanism
Isothermal thermogravimetry
Prout–Tompkins equation
Sodium oxalate

ABSTRACT

The kinetics of thermal decomposition of sodium oxalate ($Na_2C_2O_4$) has been studied as a function of concentration of dopant, aluminium, at five different temperatures in the range 783–803 K under isothermal conditions by thermogravimetry (TG). The TG data were subjected to both model fitting and model free kinetic methods of analysis. The model fitting analysis of the TG data shows that no single kinetic model describes the whole α versus t curve with a single rate constant throughout the decomposition reaction. Separate kinetic analysis shows that Prout–Tompkins model best describes the acceleratory stage of the decomposition while the decay region is best fitted with the contracting cylinder model. Activation energy values were evaluated by model fitting and model free kinetic methods for both stages of decomposition. As proposed earlier the results favours a diffusion controlled mechanism for the isothermal decomposition of sodium oxalate.

1. Introduction

Inorganic oxalates are crystalline solids with definite composition, characteristic dehydration and decomposition temperatures and kinetics. The nature of decomposition products and exact stoichiometry of decomposition are also known. This made them unique in the standardization and calibration of thermoanalytical equipments [1,2]. They are also used as standard materials in developing methods and experimental procedures for thermal dehydration and decomposition of solids [1,3–5]. For many oxalates the mechanism of thermal decomposition and dehydration are well established and are commonly used as standard substances to confirm the exactness of theoretically developed models and equations of thermal decomposition of solids [6–9].

Information about the thermal stability of solid materials of all kinds is of great practical and technological importance [1,10,11]. Thermogravimetric analysis (TG) is usually adopted to study the kinetics of thermally activated solid state reactions to obtain thermal stability parameters of solids [12–15]. The kinetics of the thermal decomposition of inorganic materials could be markedly affected by pre-treatments, by the shortening of the induction period followed by an overall decrease in time needed to complete the reaction. The thermal decomposition data generated from TG can be analysed and manipulated to obtain kinetic parameters [16–25]. Solid-state kinetic data are of practical interest for the large and growing number of technologically important processes. A number of reviews are available in the literature on these processes [26–33]. Kinetic studies predict how quickly a system approaches equilibrium and also help to understand the mechanism of the process [27,28]. Several authors have emphasized the practical and theoretical importance of information on the kinetics and mechanism of solid state decompositions [1,34].

1.1. Thermal decomposition of metal oxalates

Thermal decomposition of metal oxalates has been the subject of many researches, both from a practical and theoretical viewpoint [35–37]. The thermal decomposition and its kinetics, belonging to $Ag_2C_2O_4$, NiC_2O_4, MnC_2O_4, HgC_2O_4, PbC_2O_4, $MgC_2O_4.2H_2O$ and $SrTiO(C_2O_4)_2{\cdot}4H_2O$ [1,35,37–39] were reported. Duval [40] has summarized the thermogravimetric data for the drying and ignition temperature of a large number of metal oxalates. Galwey and Brown [41] has identified and discussed the studies on the thermal decomposition of silver oxalate. The studies on the thermal decomposition of cobalt oxalate [42] and manganese (II) oxalate dihydrate and manganese (II) oxalate trihydrate [43] using TG, differential thermal analysis (DTA) and X-ray diffraction (XRD) techniques has also been reported.

A review on the literature of the thermal behaviour of inorganic oxalates reveals that except yttrium oxalate, all undergo decomposition before melting and the decomposition kinetics are not complicated except in the case of a few. However, the kinetic

* Corresponding author. Tel.: +91 494 2401144x413; fax: +91 494 2400269.
E-mail address: devitgdevi@gmail.com (T. Ganga Devi).

0040-6031/$ – see front matter © 2012 Elsevier B.V. All rights reserved.
doi:10.1016/j.tca.2012.02.003

models proposed vary from oxalate to oxalate and author to author. The decomposition invariably involves the C—C bond breaking. Gorski and Kranicka [44] proposed that the decomposition in oxalates begins with the heterolytic dissociation of C—C bond forming CO_2 and CO_2^{2-}. The literature review reveals that no systematic studies have been carried out on oxalates except silver oxalate and to an extent nickel oxalate. The decomposition of oxalates involves the cleavage of the C—C bond, since the products are CO and CO_2 which contain only one carbon atom each. Infrared analysis proved the internal rotation of the carbonyl group about the C—C bond [45]. In many cases the C—C bond cleavage is the rate-determining step [42]. The cleavage may be heterolytic to produce CO_2 and CO_2^{2-} [44] or hemolytic to produce two CO_2^- anions [46]. In silver oxalate [47], the transfer of an electron from the $C_2O_4^{2-}$ to the cation is the first stage of the decomposition which leads to the rupture of the C—C bond [1].

1.2. Review of earlier work

Dollimore [48] has made an excellent review on the thermal decomposition and stability of many oxalates. Chaiyo et al. [49] studied the thermal decomposition of $Na_2C_2O_4$ using non-isothermal TG-DTA, XRD, and scanning electron microscopy (SEM); performed the kinetics analysis of the non-isothermal decomposition data using the iso-conversional methods, proposed by Ozawa and Kissinger–Akahira–Sunose (KAS), and possible conversion functions have been estimated by the Liqing–Donghua method [50].

1.3. Objective of the present investigation

The broad objective of our investigation is to study the role of lattice defects on solid state decomposition kinetics of alkali metal oxalates with a view to controlling the reactivity of solids in general. As solid-state reactions often occur between crystal lattices or with molecules that must permeate into lattices where motion is restricted and may depend on lattice defects [51], the solids under investigation are subjected to pretreatments such as doping, precompression, preheating, etc., to modify the magnitude and nature of lattice defects. Pretreatments such as irradiation, mechanical grinding, doping, etc., affect the rate and temperature of decomposition of oxalates [52–54]. The first two factors generally increase the rate and decrease the decomposition and dehydration temperatures. In some cases even the treatment itself brings about dehydration and decomposition [55]. The effects of pretreatments on decomposition kinetics provide valuable information regarding the topochemistry of the solid and the kinetics and mechanism of the solid state reactions.

Sodium oxalate is a colourless crystalline solid soluble in water, crystallize as anhydrous salt and undergo thermal decomposition around 773 K to carbonate [51,56]:

$$Na_2C_2O_4 \rightarrow Na_2CO_3 + CO$$

As a starting material for versatile industries, it is very important to determine the thermal decomposition mechanism, kinetics and thermodynamic parameters of sodium oxalate for advantages in cost and time management for industrial production. Although there has been increasing interest in the study of experimental factors and processing parameters, especially in determining the kinetics of thermal decomposition reactions, many features of oxalate decomposition still remain unclear. In the present paper we describe the kinetics of the thermal decomposition of Al^{3+} doped sodium oxalate.

2. Experimental

2.1. Materials

All the chemicals used in the present study were of AnalaR grade samples of E Merck. $AlCl_3{\cdot}6H_2O$ is used for doping Al^{3+}. Like earlier workers [57–62], the doped samples were prepared by the method of co-crystallization. Aluminium doped samples of sodium oxalate were prepared as per the following procedure. 10 g of sodium oxalate was dissolved in 230 ml of distilled water at boiling temperature in a 500 ml beaker. 10 ml of a solution containing the desired quantity of Al^{3+} is added to the hot solution so as to achieve a total volume of 240 ml. The solution, containing desired concentration of the dopant, was then cooled slowly to room temperature. The beaker containing the solution was covered using a clean uniformly perforated paper and kept in an air oven at a temperature of 333 K over a period of 6–7 days to allow slow crystallization by evaporation. The resulting crystals were removed; air dried, powdered in an agate mortar, fixed the particle size in the range 106–125 μm and kept in a vacuum desiccator. The doped samples were prepared at five different concentrations, viz. 10^{-5}, 10^{-4}, 10^{-3}, 10^{-2}, 10^{-1}, and 1 mol%.

2.2. Thermogravimetric analysis

Thermogravimetric measurements in static air were carried out on a custom-made thermobalance fabricated in this laboratory [59,60], a modified one of that reported by Hooley [63]. A major problem [64] of the isothermal experiment is that a sample requires some time to reach the experimental temperature. During this period of non-isothermal heating, the sample undergoes some transformations that are likely to affect the succeeding kinetics. The situation is especially aggravated by the fact that under isothermal conditions, a typical solid-state process has its maximum reaction rate at the beginning of the transformation. So we fabricated a thermobalance particularly for isothermal studies, in which loading of the sample is possible at any time after the furnace has attained the desired reaction temperature. The operational characteristics of the thermobalance are, balance sensitivity: $\pm 1 \times 10^{-5}$ g, temperature accuracy: ±0.5 K, sample mass: 5×10^{-2} g, atmosphere: static air and crucible: platinum. Thermal decomposition of sodium oxalate was found to be very slow below 783 K and very fast above 803 K. The decomposition was thus studied in the range 783–803 K. The loss in mass of sodium oxalate was measured as a function of time (t) at five different temperatures (T), viz., 783, 788, 793, 798 and 803 K.

2.3. Kinetic analysis

Both model fitting and model free methods were used for the kinetic analysis of the TG data. Historically model-fitting methods were widely used, because of their ability to directly determine the kinetic triplet involving Arrhenius parameters, for the analyses of mass loss data obtained from solid state thermal decomposition reactions. On the other hand, model free (isoconversional) methods do not compute a frequency factor nor determine reaction models which are needed for a complete and accurate kinetic analysis. In solid state kinetics, mechanistic interpretations usually involve identifying a reasonable reaction model [65] because information about individual reaction steps is often difficult to obtain. A model can describe a particular reaction type and translate that mathematically into a rate equation. Many models have been proposed in solid-state kinetics and these models have been developed based on certain mechanistic assumptions. Solid-state kinetic reactions can be mechanistically classified as

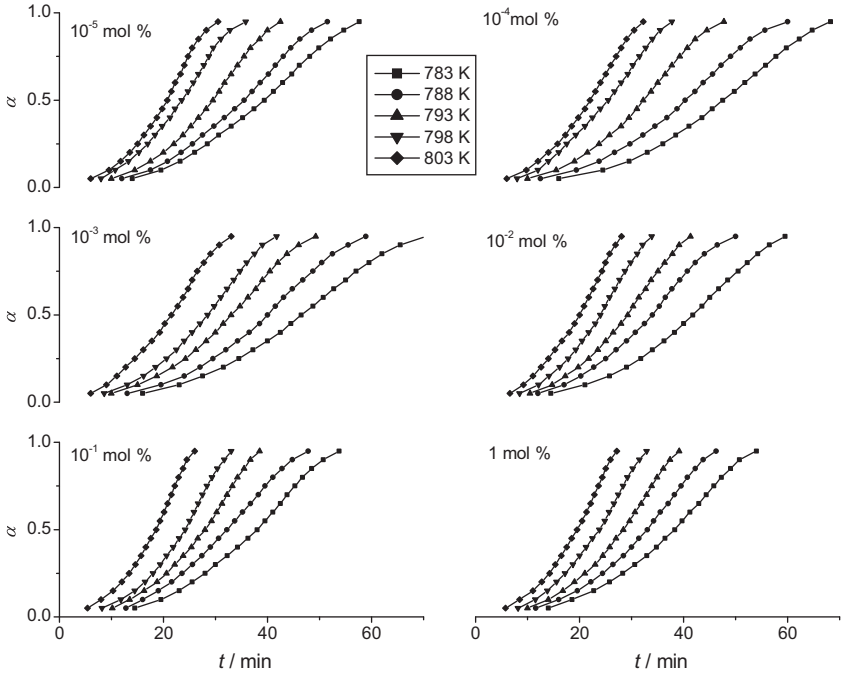

Fig. 1. α versus t plots for the thermal decomposition of aluminium doped sodium oxalate samples at different dopant concentrations. The form of this kinetic expression.

nucleation, geometrical contraction, diffusion and reaction order models [1].

Application of isoconversional methods permit model-independent estimates of the activation energy (E) related to different extents of conversion, α, without the knowledge of $g(\alpha)$. The analysis of the dependence of E on α is very instructive because it helps to disclose the complexity of the process and also to gain an insight into its mechanism.

3. Results and discussion

The experimental mass loss data obtained from TG were transformed in to α versus t data as reported earlier [62], in the range $\alpha = 0.05–0.95$ with an interval of 0.05, at all temperatures studied. The α versus t curves for the isothermal decomposition of all Al^{3+} doped sodium oxalate samples at all temperatures studied are shown in Fig. 1. The observed mass changes for the decomposition agree very well with the theoretical value at all temperatures studied. Doping with Al^{3+} did not change the basic shape (sigmoid) of the α versus t curves. The TG data were subjected to both model fitting and model free kinetic methods of analysis.

3.1. Model fitting method

The α versus t data in the range $\alpha = 0.05–0.95$ of the isothermal decomposition of Al^{3+} doped sodium oxalate samples at all

Table 1
Reaction models used in the present investigation to describe the thermal decomposition of aluminium doped sodium oxalate samples.

Model	Reaction model	Function, $g(\alpha)$
R2	Contracting cylinder	$1-(1-\alpha)^{1/2}$
R3	Contracting sphere	$1-(1-\alpha)^{1/3}$
D1	One-dimensional diffusion	α^2
D2	Two-dimensional diffusion	$(1-\alpha)\ln(1-\alpha)+\alpha$
D3	Three-dimensional diffusion	$[1-(1-\alpha)^{1/3}]^2$
D4	Ginstling–Brounshtein	$1-(2\alpha/3)-(1-\alpha)^{2/3}$
F1	First order	$-\ln(1-\alpha)$
F2	Second order	$(1-\alpha)^{-1}-1$
PT	Prout–Tompkins	$\ln[\alpha/(1-\alpha)]$

Table 2
Values of rate constants, k_1 and k_2, obtained from model fitting respectively to Prout–Tompkins model (acceleratory stage) and contracting cylinder model (decelerator stage) for the thermal decomposition of aluminium doped sodium oxalate samples.

T/K	Dopant concentration/mol%	$k_1 \times 10^3$/min	$k_2 \times 10^4$/min
783	0	1.97	4.69
	1×10^{-5}	1.78	4.23
	1×10^{-4}	1.60	3.69
	1×10^{-3}	1.52	3.41
	1×10^{-2}	1.78	4.30
	1×10^{-1}	1.92	5.00
	1	1.86	4.77
788	0	2.29	5.69
	1×10^{-5}	2.08	5.06
	1×10^{-4}	1.84	4.41
	1×10^{-3}	1.76	4.13
	1×10^{-2}	2.10	5.21
	1×10^{-1}	2.25	6.03
	1	2.16	5.77
793	0	2.65	6.82
	1×10^{-5}	2.42	6.07
	1×10^{-4}	2.14	5.25
	1×10^{-3}	2.04	4.96
	1×10^{-2}	2.41	6.30
	1×10^{-1}	2.61	7.26
	1	2.52	6.97
798	0	3.07	8.28
	1×10^{-5}	2.78	7.29
	1×10^{-4}	2.50	6.29
	1×10^{-3}	2.37	5.96
	1×10^{-2}	2.79	7.54
	1×10^{-1}	3.00	8.70
	1	2.93	8.35
803	0	3.58	9.91
	1×10^{-5}	3.22	8.69
	1×10^{-4}	2.92	7.51
	1×10^{-3}	2.78	7.15
	1×10^{-2}	3.23	9.09
	1×10^{-1}	3.53	10.50
	1	3.40	9.95

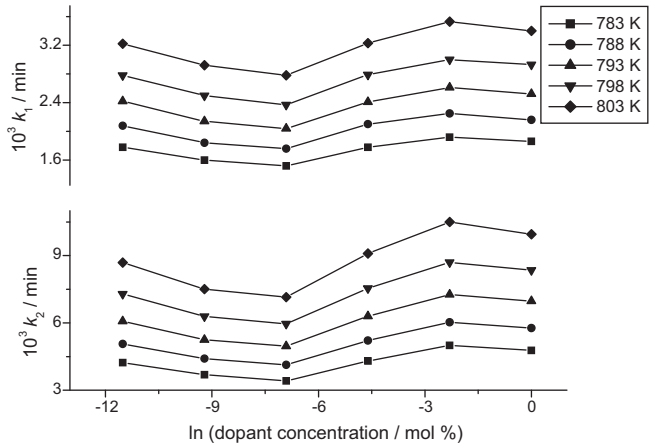

Fig. 2. Dependence of k_1 and k_2 on dopant concentration at different temperatures.

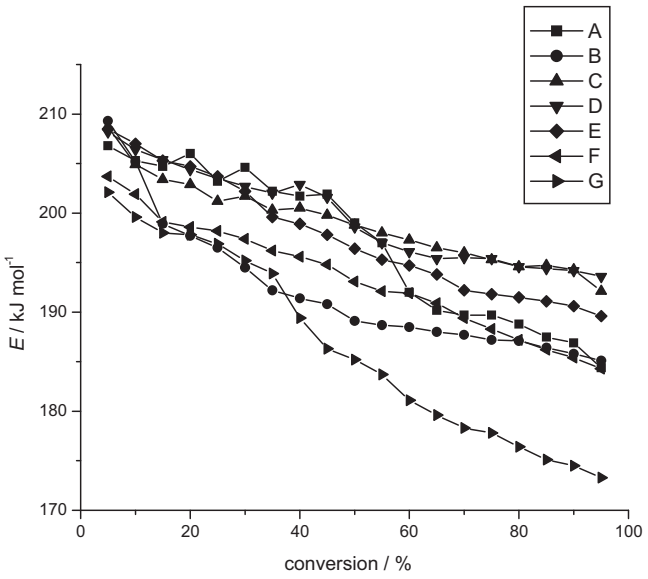

Fig. 3. Dependence of E on conversion for the thermal decomposition of undoped (A) and Al^{3+} doped (B: 10^{-5}, C: 10^{-4}, D: 10^{-3}, E: 10^{-2}, F: 10^{-1} and G: 1 mol%) sodium oxalate.

temperatures were subjected to weighted least squares analysis, as described earlier [62], to various kinetic models reported elsewhere [1]. However, only the reactions models given in Table 1 give a correlation coefficient value above 0.9 and so we have used these reaction models, for the kinetic analysis, in the present study. We found that no single kinetic equation fitted the whole α versus t data with a single rate constant throughout the reaction as observed earlier [66]. Fig. 1 shows that the isothermal decomposition of the samples undergoes through an acceleratory period (up to $\alpha = 0.5$) followed by the decelerating period. This fact prompted us to do separate kinetic analysis for the acceleratory and decelerating regions, which reveal that the region $\alpha = 0.05$–0.5 (acceleratory stage) of the TG curve is best described by Prout–Tompkins [67] model $\{\ln [\alpha/(1-\alpha)] = kt\}$ with rate constant k_1; beyond $\alpha = 0.5$, however, this model fails but fitted better to contracting cylinder model $[1-(1-\alpha)^{1/2} = kt]$ with a rate constant k_2. Such a description of reaction kinetics using different rate laws for different ranges of conversion is not unusual in solid-state reactions. For instance Philips and Taylor used Prout–Tompkins equation to describe the acceleratory region of the decomposition of potassium metaperiodate (KIO_4) and the contracting sphere equation for the decay stage [68]. It has also been reported that under isothermal conditions KIO_4 decomposes via two stages; the Prout–Tompkins equation best describes the acceleratory stage and the decelerating stage proceeds according to contracting cylinder law [59,62,69]. The acceleratory stage in the decomposition of lithium perchlorate followed Prout–Tompkins rates law whereas the decay stage followed the monomolecular model [70]. Similarly both the acceleratory and decay regions of the thermal decomposition of sodium perchlorate and of potassium bromate were well described by the Prout–Tompkins relation with separate rate constants [71]. Several other authors [72–76] have also described the reaction kinetics for the same solid using different rate laws for different ranges of α.

The values of rate constants, k_1 and k_2, obtained from model fitting method respectively to Prout–Tompkins model (acceleratory stage) and contracting cylinder model (decelerating stage) for the thermal decomposition of Al^{3+} doped sodium oxalate samples studied are presented in Table 2. The dependence of k_1 and k_2 on dopant concentration at different temperatures is shown in Fig. 2. It is observed that Al^{3+}, which produces cation vacancies in the sodium oxalate lattice, decreases the rate of the decomposition up to a dopant concentration of 10^{-2} mol%, after which the rate begins to increase slowly with further increase in dopant concentration. However, the rate remained lower than that of the undoped sodium oxalate even when the dopant concentration is increased to 1 mol%. The desensitizing effect shows the same pattern in both acceleratory and decay stage at all the five temperatures examined.

The values of E, standard deviation (SD), error and correlation coefficient (r) obtained from Arrhenius plot for the acceleratory and decelerating stages of the thermal decomposition of all Al^{3+} doped sodium oxalate samples are given in Table 3 along with the values for the undoped sodium oxalate for the purpose of comparison.

3.2. Model free method

The α versus t data, in the range of $\alpha = 0.05$–0.95, of the isothermal decomposition of all Al^{3+} doped sodium oxalate samples were also subjected to integral isoconversional kinetic studies for the determination of apparent activation energy as a function of α from the sets of isothermals obtained. A plot of ln t (t being the time

Table 3
Values of E, standard deviation (SD), error and correlation coefficient (r) obtained from the Arrhenius plot for the acceleratory and decelerator stages of the thermal decomposition of aluminium doped sodium oxalate samples.

Dopant concentration/mol%	Acceleratory stage ($\alpha = 0.05 - 0.5$)				Deceleratory stage ($\alpha = 0.5 - 0.95$)			
	E/kJ/mol^{-1}	SD	Error	$-r$	E/kJ/mol^{-1}	SD	Error	$-r$
Nil	155.5	0.0038	0.1494	0.9999	195.7	0.0036	0.1445	0.9999
10^{-5}	154.3	0.0041	0.1615	0.9999	188.7	0.0025	0.0995	1.0000
10^{-4}	157.8	0.0078	0.3112	0.9996	185.7	0.0034	0.1352	1.0000
10^{-3}	157.3	0.0066	0.2626	0.9997	193.2	0.0015	0.0592	1.0000
10^{-2}	154.3	0.0064	0.2551	0.9997	195.2	0.0025	0.1002	1.0000
10^{-1}	157.4	0.0068	0.2692	0.9997	193.5	0.0028	0.1101	1.0000
1	158.0	0.0019	0.0754	1.0000	192.4	0.0036	0.1413	0.9999

required for reaching a given value of α at a constant temperature T) versus the corresponding reciprocal of the temperature ($1/T$) would lead to the activation energy for the given value of α. The values of activation energy obtained through isoconversional method for the thermal decomposition of Al^{3+} doped sodium oxalate at different conversions are given in Table 4 and the dependence of E on conversion is shown in Fig. 3. Table 4 reveals that the activation energy values obtained for different conversions corresponding to the acceleratory period are higher than those obtained for the deceleratory stage of the thermal decomposition of sodium oxalate. Examination of Fig. 3 reveals that the values of E are independent of conversion above 50%; however, below 50% the E values depend on conversion. This implies that the pretreatment affects the nucleation and its growth in the solid. Once the decay starts, i.e., after the completion of nucleation and its growth, the decomposition process continues with a steady decrease in the value of E till the end of the process. It is observed that the activation energy for the thermal decomposition of Al^{3+} doped sodium oxalate with a dopant concentration of 1 mol% shows more than 10% decrease from the values obtained for other samples studied, which is attributed to the high concentration of defects present in the lattice.

3.3. Mechanism of decomposition

Diffusion of the cation and/or the anion towards the potential sites, where they can react, usually determines the reaction rate of solid state decompositions. Migration of ions is greatly influenced by the defect structure of the solid. Since the size of the cation is significantly smaller than that of the anion in the oxalate systems, Frenkel defect structure is expected to dominate in these solids. For instance, silver oxalate has been shown to have Frenkel defect structure [1]. No such literature is available on sodium oxalate. However, from size considerations (Na^+ is much smaller than Ag^+), it may be assumed that sodium oxalate is also a solid with Frenkel defect structure.

Diffusion of ions can occur mainly in two ways; vacancy mechanism and interstitial mechanism. Both will have their own contributions, but depending upon the characteristic of the solid one may dominate over the other. Due to larger size, migration of $C_2O_4^{2-}$ will be negligible in comparison with Na^+ and hence the rate of oxalate decomposition will be controlled by diffusion of cation. The possible diffusion processes taking place during the thermal decomposition of sodium oxalate, diffusion of Na^+ ions occupying normal lattice sites and diffusion of Na^+ ions occupying the interstitial sites, will be greatly affected by a change in the concentration of defects leading to a complex reactivity of the solid.

Doping of sodium oxalate with Al^{3+} result in the generation of a maximum of five cation vacancies (one cation vacancy is generated per each Cl^- ion introduced) in the sodium oxalate lattice. Thus doping results in an increase in the concentration of cation vacancies and we observed, in the present investigation, that doping with Al^{3+} ions results in a decrease of the rate of thermal decomposition (Table 2 and Fig. 2). We also observed that the decrease, at lower concentrations, in the rate of decomposition caused by the dopant Al^{3+} is greater than that caused by the dopant Ba^{2+} [77]. As the product of the concentration of cation vacancy and interstitial being a constant, an increase in the concentration of cation vacancies results in a decrease of the concentration of Na^+ interstitials. This is due to the sucking in [78] of interstitials to the normal lattice sites. The decrease in the concentration of interstitials and filling up of vacancies by these vanishing interstitials result in a decrease of the diffusion rate of cation, and thereby the decomposition rate. This accounts for the initial decrease of decomposition rate.

But when the sucking of interstitials into the normal vacant lattice sites is complete, further increase in the concentration of dopants results in a sudden increase in the concentration of cation

Table 4
Values of E, standard deviation (SD) and r obtained through the integral isoconversional method for the thermal decomposition of Al^{3+} doped sodium oxalate at different conversions.

Conversion/%	Dopant concentration/mol%																	
	10^{-5}			10^{-4}			10^{-3}			10^{-2}			10^{-1}			1		
	E/kJ mol^{-1}	SD	r	E/kJ mol^{-1}	SD	r	E/kJ mol^{-1}	SD	r	E/kJ mol^{-1}	SD	r	E/kJ mol^{-1}	SD	r	E/kJ mol^{-1}	SD	r
10	205.2	0.0571	0.9871	204.9	0.0110	0.9997	206.4	0.0653	0.9879	207.0	0.0412	0.9936	201.9	0.0790	0.9791	199.6	0.0638	0.9834
20	197.7	0.0498	0.9879	202.9	0.0385	0.9956	204.4	0.0725	0.9839	204.7	0.0335	0.9959	198.6	0.0634	0.9814	197.8	0.0258	0.9968
30	194.5	0.0458	0.9889	201.7	0.0460	0.993	202.7	0.0621	0.9862	202.2	0.0284	0.9968	197.4	0.0511	0.9870	195.2	0.0304	0.9954
40	191.4	0.0373	0.9925	200.5	0.0378	0.9951	202.9	0.0427	0.9928	198.9	0.0165	0.9988	195.6	0.0492	0.9881	189.4	0.0240	0.9971
50	189.1	0.0375	0.9927	198.8	0.0269	0.9973	198.6	0.0439	0.9919	196.4	0.0137	0.9992	193.1	0.0428	0.9908	185.2	0.0224	0.9973
60	188.5	0.0327	0.9946	197.3	0.0228	0.9980	196.1	0.0381	0.9937	194.7	0.0141	0.9991	191.9	0.0382	0.9928	181.1	0.0186	0.9981
70	187.7	0.0325	0.9946	196.0	0.0233	0.9979	195.5	0.0396	0.9934	192.2	0.0148	0.9990	189.4	0.0374	0.9932	178.3	0.0182	0.9982
80	187.1	0.0314	0.9952	194.6	0.0227	0.9980	194.6	0.0342	0.9950	191.5	0.0147	0.9990	187.2	0.0384	0.9930	176.4	0.0164	0.9985
90	185.8	0.0256	0.9967	194.3	0.0267	0.9972	194.2	0.0251	0.9973	190.6	0.0070	0.9998	185.4	0.0413	0.9922	174.5	0.0187	0.9981

vacancies, which promote the diffusion of Na^+. This amounts to an increase of decomposition rate and accounts for the increase of rate observed at higher concentrations. Boldyrev [79] demonstrated the sucking of interstitials in silver oxalate by doping it with Cd^{2+}. They observed that the conductance of silver oxalate was considerably decreased by doping with Cd^{2+}. The cation vacancies generated in the silver oxalate lattice by doping suck the interstitial Ag^+ ions to the normal lattice sites thereby reducing the interstitial diffusion and thus the conductance. They also observed that when the Cd^{2+} doping is excessive (more than 1.5 mol%), the interstitial concentration becomes so low that conduction via vacancy mechanism becomes prominent. Silver halides doped with Cd^{2+} [80] and sodium nitrite doped with Ba^{2+} [81] also showed decrease in conductivity due to similar reasons.

4. Conclusions

The thermal decomposition and kinetics of sodium oxalate as a function of dopant, Al^{3+}, concentration is investigated by thermogravimetric analysis in the temperature range 783–803 K under isothermal conditions. We observed that no single kinetic equation fitted the whole α versus t curve with a single rate constant throughout the reaction. Separate kinetic analysis of the α versus t data of acceleratory ($\alpha = 0.05 - 0.5$) and decelerator ($\alpha = 0.5 - 0.95$) stages of the thermal decomposition reveal that the acceleratory stage is best fitted with Prout–Tompkins model (a model developed on the assumption of branching nucleation) and the contracting cylinder model (a model in which the advancement of interface into the bulk of the reactant particle proceeds only from the edges of the crystal surfaces upon which nucleation occurs or simply speaking the inward movement of the interface is two dimensional/cylindrical in nature) best describes the deceleratory stage. The correspondence of acceleratory stage of the decomposition with Prout–Tompkins model indicates that the nucleus growth takes place by propagation of chains. The decrease of the rate in the decay period is likely to be due to the merging of these chains, leading to the kinetics in accordance with the contracting cylinder model. The observed decrease in the decomposition rate, at lower dopant concentrations, is explained on the basis of the sucking in of Na^+ interstitials to the normal lattice sites, while the increase at higher dopant concentrations is accounted by the sudden increase in the concentration of cation vacancies.

The kinetic results obtained from the integral isoconversional method, for the entire range of conversion ($\alpha = 0.05 - 0.95$) of the thermal decomposition of Al^{3+} doped sodium oxalate samples, shows that the values of E are independent of conversion above 50%; however, below 50% the E values depend on conversion. This implies that the pretreatment affects the nucleation and its growth in the solid. Once the decay starts, i.e., after the completion of nucleation and its growth, the decomposition process continues with a steady decrease in the value of E till the end of the process. We observed that the activation energy for the thermal decomposition of Al^{3+} doped sodium oxalate with a dopant concentration of 1 mol% shows lower values (more than 10%) than the values obtained for other samples studied, which is attributed to the high concentration of defects present in the lattice. The observed change in rate of decomposition with dopant concentration could not be explained on the basis of electron transfer or bond breaking but favours a diffusion controlled mechanism for the thermal decomposition of sodium oxalate.

References

[1] A.K. Galwey, M.E. Brown, Thermal Decomposition of Ionic Solids, Elsevier, Amsterdam, 1999.
[2] P.M. Madhusudanan, K. Krishnan, K.N. Ninan, Thermal analysis, Vol. 2: Proceedings of the Seventh International Conference on Thermal Analysis, 1982, p. 226.
[3] E. Urbanovici, E. Segal, The heating rate as a variable in non-isothermal kinetics: II. A method to evaluate the non-isothermal kinetic parameters using this principle and integration over low ranges of variables, Thermochim. Acta 107 (1986) 353–357.
[4] J. Moll, D. Kerug, D. Lept, Thermal analysis, Vol. 1: Proceedings of the Sixth International Conference on Thermal Analysis, 1980, p. 57.
[5] E. Urbanovici, E. Segal, On a new classical method to evaluate non-isothermal kinetic parameters, Thermochim. Acta 107 (1986) 359–363.
[6] E. Urbanovici, E. Segal, New equations in non-isothermal kinetics taking into account the dependences A(α) and E(α), Thermochim. Acta 98 (1986) 385–390.
[7] K. Krishnan, K.N. Ninan, P.M. Madhusudanan, Computation of activation energy spectrum – a new approach, Thermochim. Acta 101 (1986) 365–371.
[8] E.S. Freeman, B. Carroll, The application of thermoanalytical techniques to reaction kinetics: the thermogravimetric evaluation of the kinetics of the decomposition of calcium oxalate monohydrate, J. Phys. Chem. 62 (1958) 394–397.
[9] E.L. Simons, A.E. Newkirk, New studies on calcium oxalate monohydrate: a guide to the interpretation of thermogravimetric measurements, Talanta 11 (1964) 549–571.
[10] K.H. Stern, High Temperature Properties and Thermal Decomposition of Inorganic Salts with Oxy Anions, CRC Press LLC, Florida, 2001.
[11] S. Vyazovkin, Thermal analysis, Anal. Chem. 76 (2004) 3299–3312.
[12] C. Deng, J. Cai, R. Liu, Kinetic analysis of solid state reactions: evaluation of approximations to temperature integral and their applications, Solid State Sci. 11 (2009) 1375–1379.
[13] Y. Huang, Y. Cheng, K. Alexander, D. Dollimore, The thermal analysis study of the drug captopril, Thermochim. Acta 367 (2001) 43–58.
[14] D. Dollimore, C. O'Connell, A comparison of the thermal decomposition of preservatives, using thermogravimetry and rising temperature kinetics, Thermochim. Acta 324 (1998) 33–48.
[15] I. Halikia, P. Neou-Syngouna, D. Kolitsa, Isothermal kinetic analysis of the thermal decomposition of magnesium hydroxide using thermogravimetric data, Thermochim. Acta 320 (1998) 75–88.
[16] S. Vyazovkin, C.A. Wight, Model-free and model-fitting approaches to kinetic analysis of isothermal and nonisothermal data, Thermochim. Acta 340–341 (1999) 53–68.
[17] M.E. Brown, Introduction to Thermal Analysis: Techniques and Applications, 2nd ed., Kluwer Academic Publishers, The Netherlands, 2001.
[18] M.A. Gabal, A.A. El-Bellihi, H.H. El-Bahnasawy, Non-isothermal decomposition of zinc oxalate–iron(II) oxalate mixture, Mater. Chem. Phys. 81 (2003) 174–182.
[19] J. Garcia-Guinea, V. Correcher, E. Lozano-Diz, M.A. Bañares, P. Lopez-Arce, A.M. García, D.A. Moreno, Effect of thermal annealing on synthetic sodium oxalate crystals, J. Anal. Appl. Pyrolysis 91 (2011) 332–337.
[20] E. Lamprecht, G.M. Watkins, M.E. Brown, The thermal decomposition of copper(II) oxalate revisited, Thermochim. Acta 446 (2006) 91–100.
[21] H. Tanaka, Thermal analysis and kinetics of solid state reactions, Thermochim. Acta 267 (1995) 29–44.
[22] A. Perejón, P.E. Sánchez-Jiménez, J.M. Criado, L.A. Pérez-Maqueda, Kinetic analysis of complex solid-state reactions. A new deconvolution procedure, J. Phys. Chem. 115B (2011) 1780–1791.
[23] J. Cai, R. Liu, Y. Wang, Kinetic analysis of solid-state reactions: a new integral method for nonisothermal kinetics with the dependence of the preexponential factor on the temperature ($A = A_0 T^n$), Solid State Sci. 9 (2007) 421–428.
[24] J. Cai, R. Liu, Kinetic analysis of solid-state reactions: precision of the activation energy obtained from one type of integral methods without neglecting the low temperature end of the temperature integral, Solid State Sci. 10 (2008) 659–663.
[25] J. Málek, T. Mitsuhashi, J.M. Criado, Kinetic analysis of solid-state processes, J. Mater. Res. 16 (2001) 1862–1871.
[26] V.A. Benderskii, D.E. Makarov, C.A. Wight, Chemical Dynamics at Low Temperatures, Wiley, New York, 1994, p. 385.
[27] M.E. Brown, D. Dollimore, A.K. Galwey, Reactions in the Solid State, Comprehensive Chemical Kinetics, vol. 22, Elsevier, Amsterdam, 1980, p. 340.
[28] S. Vyazovkin, C.A. Wight, Isothermal and nonisothermal reaction kinetics in solids: in search of ways toward consensus, J. Phys. Chem. 101A (1997) 8279–8284.
[29] T.B. Brill, K.J. James, Kinetics and mechanisms of thermal decomposition of nitroaromatic explosives, Chem. Rev. 93 (1993) 2667–2692.
[30] H.F. Mark, N.M. Bikales, C.G. Overberger, G. Menges (Eds.), Encyclopedia of Polymer Science and Engineering, Wiley, New York, 1989, p 231 & 690.
[31] S. Vyazovkin, C.A. Wight, Isothermal and nonisothermal kinetics of thermally stimulated reactions of solids, Int. Rev. Phys. Chem. 17 (1998) 407–433.
[32] D. Dollimore, Thermal analysis, Chem. Rev. 68 (1996) 63–72.
[33] A.K. Galwey, Is the science of thermal analysis kinetics based on solid foundations?: a literature appraisal, Thermochim. Acta 413 (2004) 139–183.
[34] S. Vyazovkin, Kinetic concepts of thermally stimulated reactions in solids: a view from a historical perspective, Int. Rev. Phys. Chem. 19 (2000) 45–60.
[35] B.V. L'vov, Kinetics and mechanism of thermal decomposition of nickel, manganese, silver, mercury and lead oxalates, Thermochim. Acta 364 (2000) 99–109.
[36] H.S.G. Murhty, M.S. Rao, T.R.N. Kutty, Thermal decomposition of titanyl oxalates—II: kinetics of decomposition of barium titanyl oxalate, J. Inorg. Nucl. Chem. 7 (1975) 1875–1878.

[37] B.S. Patra, S. Otta, S.D. Bhattamisra, A kinetic and mechanistic study of thermal decomposition of strontium titanyl oxalate, Thermochim. Acta 441 (2006) 84–88.
[38] L. Vlaev, N. Nedelchev, K. Gyurova, M. Zagorcheva, A comparative study of non-isothermal kinetics of decomposition of calcium oxalate monohydrate, J. Anal. Appl. Pyrolysis 81 (2008) 253–262.
[39] J.J. Zhang, N. Ren, J.H. Bai, Non-isothermal decomposition reaction kinetics of the magnesium oxalate dehydrate, Chin. J. Chem. 24 (2006) 360–364.
[40] C. Duval, Inorganic Thermogravimetric Analysis, 2nd ed., Elsevier, Amsterdam, The Netherlands, 1963.
[41] A.K. Galwey, M.E. Brown, An appreciation of the chemical approach of V. V. Boldyrev to the study of the decomposition of solids, J. Therm. Anal. Calorim. 90 (2007) 9–22.
[42] S. Majumdar, I.G. Sharma, A.C. Bidaye, A.K. Suri, A study on isothermal kinetics of thermal decomposition of cobalt oxalate to cobalt, Thermochim. Acta 473 (2008) 45–49.
[43] B. Donkova, D. Mehandjiev, Mechanism of decomposition of manganese(II) oxalate dihydrate and manganese(II) oxalate trihydrate, Thermochim. Acta 421 (2004) 141–149.
[44] A. Górski, A.D. Kraśnicka, The importance of the CO_2^{2-} anion in the mechanism of thermal decomposition of oxalates, J. Therm. Anal. Calorim. 32 (1987) 1229–1241.
[45] F.E. Freeberg, K.O. Hartman, I.C. Hisatsune, J.M. Schempf, Kinetics of calcium oxalate pyrolysis, J. Phys. Chem. 71 (1967) 397–402.
[46] M.V.V.S. Reddy, K.V. Lingam, T.K.G. Rao, Radical studies in oxalate systems: E.S.R. of CO_2^- in irradiated potassium oxalate monohydrate, Mol. Phys. 42 (1981) 1267–1269.
[47] A.G. Leiga, Decomposition of silver oxalate. II. Kinetics of the thermal decomposition, J. Phys. Chem. 70 (1966) 3260–3267.
[48] D. Dollimore, The thermal decomposition of oxalates. A review, Thermochim. Acta 117 (1987) 331–363.
[49] N. Chaiyo, R. Muanghlua, S. Niemcharoen, B. Boonchom, P. Seeharaj, N. Vittayakorn, Non-isothermal kinetics of the thermal decomposition of sodium oxalate $Na_2C_2O_4$, J. Therm. Anal. Calorim. 107 (2012) 1023–1029.
[50] L. Liqing, C. Donghua, Application of iso-temperature method of multiple rate to kinetic analysis, J. Therm. Anal. Calorim. 78 (2004) 283–293.
[51] D. Dollimore, D. Tinsley, The thermal decomposition of oxalates. Part XII. The thermal decomposition of lithium oxalate, J. Chem. Soc. A (1971) 3043–3046.
[52] C. Sciora, J.C. Mutin, Traitement mecanique des materiaux III Consequences du broyage sur la reactivite ulterieure de quelques hydrates, J. Therm. Anal. Calorim. 20 (1981) 125–139.
[53] C. Sciora, J.C. Mutin, Traitement mecanique des materiaux I – Modification de Phases que provoque le broyage application au cas d'une serie d'oxalates hydrates, J. Therm. Anal. Calorim. 19 (1980) 365–376.
[54] M. Rossberg, E.F. Khairetdinov, E. Linke, V.V. Boldyrev, Effect of mechanical pretreatment on thermal decomposition of silver oxalate under nonisothermal conditions, J. Solid State Chem. 41 (1982) 266–271.
[55] E. Greenberg, J.L. Settle, W.N. Hubbard, Fluorine bomb calorimetry. IV. The heats of formation of titanium and hafnium tetrafluorides, J. Phys. Chem. 66 (1962) 1345–1348.
[56] G.A. Jeffrey, G.S. Parry, The crystal structure of sodium oxalate, J. Am. Chem. Soc. 76 (1954) 5283–5286.
[57] J.N. Maycock, V.R. Pai Verneker, Role of point defects in the thermal decomposition of ammonium perchlorate, Proc. R. Soc. Lond. 307A (1968) 303–315.
[58] V.V. Boldyrev, V.V. Alexandrov, A.V. Boldyreva, V.I. Gritsan, Yu.Ya. Karpenko, O.P. Korobeinitchev, V.N. Panfilov, E.F. Khairetdinov, On the mechanism of the thermal decomposition of ammonium perchlorate, Combust. Flame 15 (1970) 71–77.
[59] M.P. Kannan, K. Muraleedharan, Kinetics of thermal decomposition of sulphate-doped potassium metaperiodate, Thermochim. Acta 158 (1990) 259–266.
[60] K. Muraleedharan, M.P. Kannan, Effects of dopants on the isothermal decomposition kinetics of potassium metaperiodate, Thermochim. Acta 359 (2000) 161–168.
[61] K. Muraleedharan, M.P. Kannan, T. Gangadevi, Thermal decomposition of potassium metaperiodate doped with trivalent ions, Thermochim. Acta 502 (2010) 24–29.
[62] V.M. Abdul Mujeeb, K. Muraleedharan, M.P. Kannan, T. Ganga Devi, Influence of trivalent ion dopants on the thermal decomposition kinetics of potassium bromate, Thermochim. Acta 525 (2011) 150–160.
[63] J.G. Hooley, A recording vacuum thermobalance, Can. J. Chem. 35 (1957) 374–380.
[64] S. Vyazovkin, C.A. Wight, Kinetics in solids, Annu. Rev. Phys. Chem. 48 (1997) 125–149.
[65] M.E. Brown, Stocktaking in the kinetic cupboard, J. Therm. Anal. Calorim. 82 (2005) 665–669.
[66] J.J. Mallikassery, K., Muraleedharan, M.P., Kannan, T. Ganga Devi, Thermal decomposition and kinetics of sodium oxalate, J. Serb. Chem. Soc., Submitted for publication.
[67] E.G. Prout, F.C. Tompkins, The thermal decomposition of potassium permanganate, Trans. Faraday Soc. 40 (1944) 488–497.
[68] B.R. Philips, D. Taylor, Thermal decomposition of potassium metaperiodate, J. Chem. Soc. (1963) 5583–5590.
[69] K. Muraleedharan, M.P. Kannan, T. Gangadevi, Effect of metal oxide additives on the thermal decomposition kinetics of potassium metaperiodate, J. Therm. Anal. Calorim. 100 (2010) 177–182.
[70] M.M. Markowitz, D.A. Boryta, The decomposition kinetics of lithium perchlorate, J. Phys. Chem. 65 (1961) 1419–1424.
[71] F. Solymosi, Structure and Stability of Salts of Halogen Oxyacids in the Solid Phase, John Wiley & Sons, London, 1977.
[72] R.A.W. Hill, A diffusion chain theory of the decomposition of inorganic solids, Trans. Faraday Soc. 54 (1958) 685–690.
[73] S.R. Mohanty, D. Patnaik, Effects of admixtures of potassium bromide on the thermal decomposition of potassium bromate, J. Therm. Anal. Calorim. 35 (1989) 2153–2159.
[74] B.C. Das, D. Patnaik, Effect of anion doping on the thermal decomposition of potassium bromate, J. Therm. Anal. Calorim. 61 (2000) 879–883.
[75] M.P. Kannan, V.M. Abdul Mujeeb, Effect of dopant ion on the kinetics of thermal decomposition of potassium bromate, React. Kinet. Catal. Lett. 72 (2001) 245–252.
[76] K. Muraleedharan, V.M. Abdul Mujeeb, M.H. Aneesh, T. Ganga Devi, M.P. Kannan, Effect of pre-treatments on isothermal decomposition kinetics of potassium metaperiodate, Thermochim. Acta 510 (2010) 160–167.
[77] M. Jose John, K. Muraleedharan, M.P. Kannan, V.M. Abdul Mujeeb, Kinetic studies on the thermal decomposition of sodium oxalate doped with barium, J. Serb. Chem. Soc., Submitted for publication.
[78] J.E. Spice, Chemical Binding and Structure, Pergamon Press, New York, 1964.
[79] V.V Boldyrev, Control of the reactivity of solids, Annu. Rev. Mater. Sci. 9 (1979) 455–469.
[80] R.J. Friaud, Ionic conductivity of thallium chloride, J. Phys. Chem. Solids 18 (1961) 203–206.
[81] C. Ramasastry, Y.V.G.S. Murti, Electrical conductivity in sodium nitrate crystals, Proc. Roy. Soc. A 305 (1968) 441–455.